

Figure S1. Related to Figure 1.

- A. Genomic distribution of NPAS4 binding sites compared to the distribution of annotations by size across the genome.
- B. ChIP-seq signal for NPAS4 binding sites in alternating unstimulated and stimulated control (left two panels) or *Npas4* shRNA-transduced neuronal cultures (right two panels). Data sorted by descending NPAS4 binding strength. Each NPAS4 binding site is represented as a single horizontal line (blue) centered at the peak summit with flanking 2kb regions. Color denotes ChIP-seq signal intensity (displayed in $\log_2(\text{counts per million} + 1)$).
- C. Venn diagram of the overlap between H3K27ac-positive sites and ATAC-seq-positive sites in cultured cortical neurons. The set of regulatory regions examined in the manuscript includes those 31,138 sites with overlapping H3K27ac and ATAC-seq signal.
- D. H3K27ac \log_2 -fold change between depolarized *Npas4*^{fl/fl} neurons infected with Cre compared to neurons infected with GFP (control) plotted by quantiles of NPAS4 binding strength at promoter regions ($1 < 4$). – indicates sites with no NPAS4 binding. *** indicates p-value < 0.001 in a Wilcoxon rank sum test comparing the fold change distribution for a given quantile relative to non-bound sites.
- E. H3K27ac \log_2 -fold change between unstimulated neurons overexpressing NPAS4 compared to unstimulated neurons overexpressing GFP (control) plotted by quantiles of NPAS4 binding strength at promoter regions ($1 < 4$, – indicates sites not bound by NPAS4). *** indicates p-value < 0.001 in a Wilcoxon rank sum test comparing the fold change distribution for a given quantile relative to non-bound sites.
- F. Luciferase activity (ratio of luciferase/renilla) of NPAS4-bound regulatory regions in KCl-depolarized neurons transfected with control shRNA or *Npas4* shRNAs. Numbers indicate the regulatory region number (see Table S1 for genomic coordinates) and are sorted into regions where NPAS4 binds with high confidence (Strong) versus low confidence (Weak). Data are plotted as the mean \pm SEM of at least 3 independent replicates. * $p < 0.05$, paired, one-sided t-test with Benjamini-Hochberg multiple hypothesis correction.
- G. Expression of marker gene *Olig1* identifies oligodendrocyte cluster in t-SNE representation of primary cortical and hippocampal culture single-cell RNA-seq data.
- H. Expression of marker gene *Neurod2* identifies excitatory neuron cluster in t-SNE representation of primary cortical and hippocampal culture single-cell RNA-seq data.
- I. Expression of marker gene *Gad2* identifies inhibitory neuron cluster in t-SNE representation of primary cortical and hippocampal culture single-cell RNA-seq data.
- J. Expression of marker gene *Aldoc* identifies astrocyte cluster in t-SNE representation of primary cortical and hippocampal culture single-cell RNA-seq data.
- K. Primary cortical and hippocampal neuronal cultures show co-clustering by cell type rather than tissue of origin in t-SNE space, suggesting similar transcriptional profiles between cell types originating from these two tissues.
- L. Heatmap of transcript counts of bHLH-PAS transcription factors in all cell types identified in previously published single-cell RNA-seq dataset from visual cortex (Hrvatin et al., 2018).

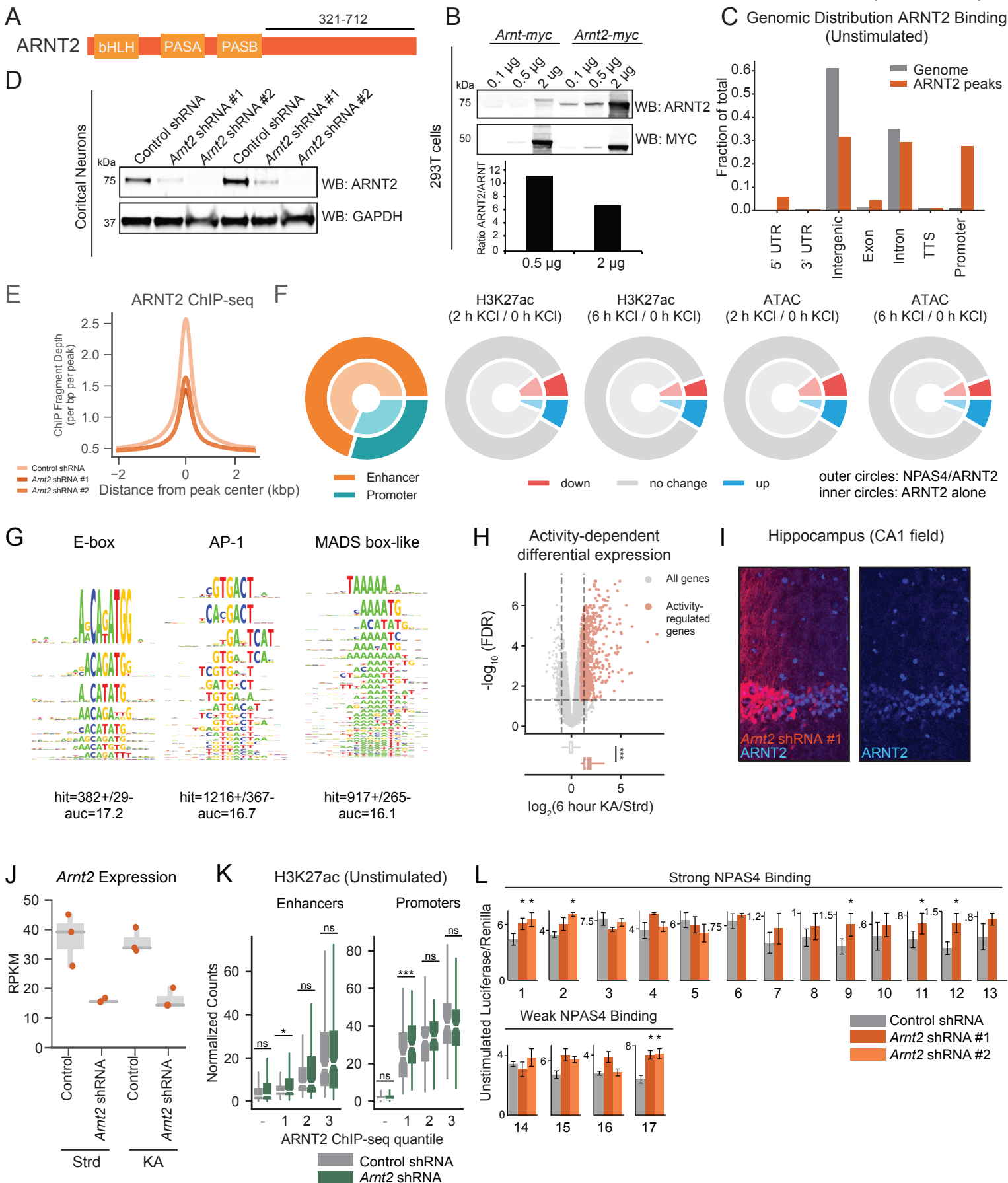


Figure S2. Related to Figure 2.

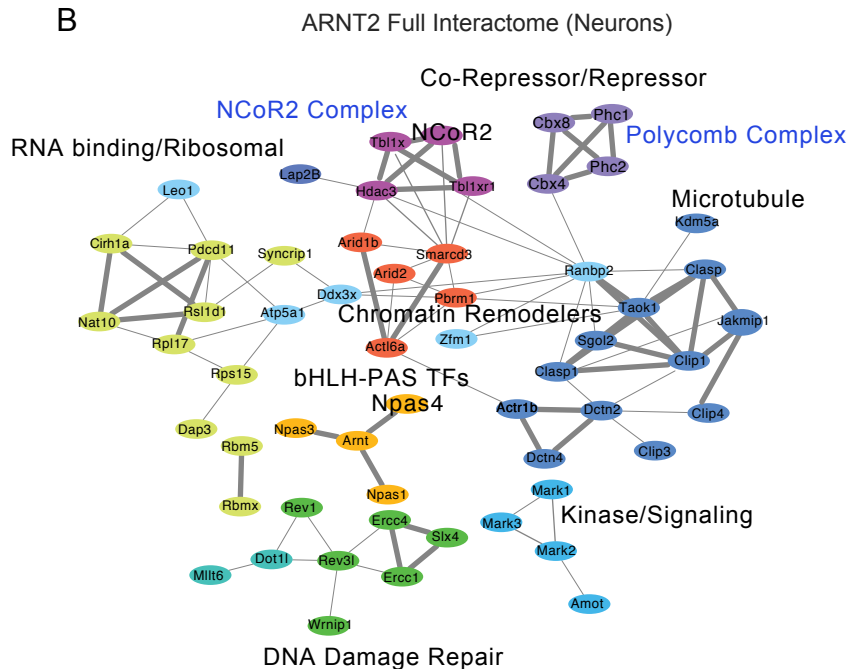
- A. ARNT2 protein domain scheme indicates C-terminal region used to generate the anti-ARNT2 antibody used in this study.
- B. Western blot analysis of the specificity and sensitivity of the anti-ARNT2 antibody against ARNT2 and the related transcription factor ARNT. Lysates were obtained from 293T cells transfected with increasing concentrations of plasmids expressing Myc-tagged ARNT2 and Myc-tagged ARNT, transferred to a membrane, and probed with anti-ARNT2 antibody (top panel). Bottom panel displays anti-ARNT2 antibody signal intensity for ARNT2-expressing lysates divided by anti-ARNT2 antibody signal intensity for ARNT-expressing lysates, at two concentrations of plasmid transfection.
- C. Genomic distributions of ARNT2 ChIP-seq binding sites from unstimulated neurons (0 hr KCl) compared to the distribution of annotations by size across the genome.
- D. Validation of *Arnt2* shRNAs by Western blot analysis of cortical neurons transduced with shRNAs targeting *Arnt2*.
- E. Mean ARNT2 ChIP-Seq signal at ARNT2 binding sites in neurons transduced with lentiviruses expressing control (non-targeting) shRNA, *Arnt2* shRNA #1, and *Arnt2* shRNA #2.
- F. Pie chart representations of NPAS4-positive/ARNT2-positive (outer circles) and NPAS4-negative/ARNT2-positive (inner circles) regulatory elements across the following categories: enhancer/promoter, direction of significant (FC > 1.5, FDR < .05) change in H3K27ac ChIP-seq (2 hr KCl, 6 hr KCl), and direction of significant change in ATAC-seq (2 hr KCl, 6 hr KCl).
- G. KSM representation of top NPAS4-positive/ARNT2-positive sites compared against top NPAS4-negative/ARNT2-positive sites reveal an enrichment of E-box, AP-1, and MADS box-like transcription factor motifs.
- H. Upper panel: $-\log_{10}(\text{false discovery rate (FDR)})$ versus \log_2 fold change in gene expression comparing hippocampi isolated from kainate-stimulated animals to saline-injected controls. Activity-regulated genes (pink) were defined as fold change >1.5 and FDR <0.05. Lower panel: Distribution of \log_2 fold changes for gene expression of all genes (gray) versus activity-dependent genes (pink). *** p = 0, Wilcoxon rank-sum test.
- I. Image of CA1 layer of the hippocampus infected with AAV virus expressing *Arnt2* shRNA-mCherry (red) and stained for expression of ARNT2 (blue) shows specific ARNT2 depletion.
- J. RPKM values for *Arnt2* in *Arnt2* shRNA or control shRNA-infected hippocampus under standard housing conditions or following injection with glutamate agonist kainate.
- K. Normalized H3K27ac ChIP-seq signal at activity-dependent, presumptive NPAS4 binding sites (enhancers and promoters, left and right respectively) in control versus *Arnt2* shRNA-treated, unstimulated cultured neurons (0 KCl). Sites have been divided into bins based on the strength of ARNT2 binding in unstimulated control neurons (3 > 1). – indicates sites with no binding. P-values were calculated comparing the distribution of H3K27ac signal in control versus *Arnt2* shRNA-treated neurons using the Wilcoxon signed-rank test. *** p < .001, * p < .05.
- L. Luciferase activity (ratio of luciferase/renilla) of NPAS4-bound regulatory regions in unstimulated neurons (0 KCl) transfected with control shRNA or *Arnt2* shRNAs. Numbers indicate the regulatory region number (see Table S1 for genomic coordinates) and are sorted into regions where NPAS4/ARNT2 bind with high confidence (Strong) versus low confidence (Weak). Data are plotted as the mean \pm SEM of at least 3 independent replicates. * p < 0.05, paired, one-sided t-test with Benjamini-Hochberg multiple hypothesis correction.

A

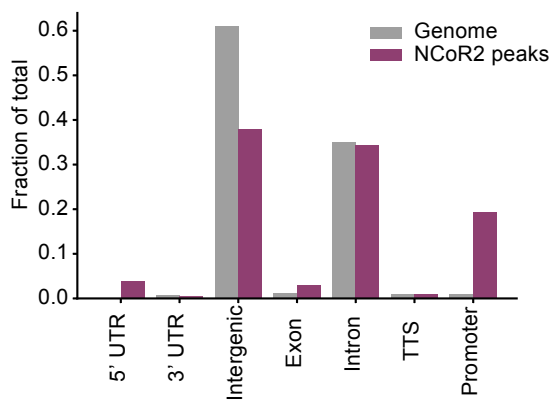
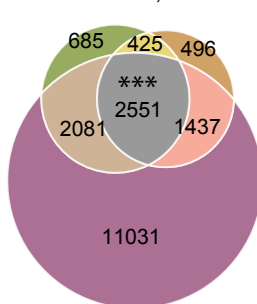
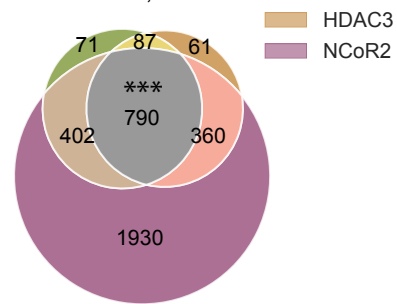
Top Ranked IP-MS ARNT2 Interactors
(Unstimulated Neurons)

Gene Symbol	MWT(kDa)	Unique Peptides	Total Peptides
Clasp2	140.65	58	149
Arnt2	77.85	39	92
Clasp1	169.12	45	71
Npas3	100.4	29	66
Ncor2	269.64	24	28
Znf318	228.08	24	24
Dync1h1	531.71	21	21
Ctip1	155.72	18	21
Ranbp2	340.91	17	21
Slx4	172.3	16	17
Erh	12.25	2	16
Ctip4	75.74	13	15
Slx4ip	45.71	9	15
Cbx8	39.84	10	13
Spats2	58.92	11	13
Tmpo	75.12	11	13
Trim33	123.76	10	12
Mark2	86.25	9	10
Rpl4	47.12	5	10
Eef1a1	50.08	6	9
Mark3	84.34	8	9
Ccar1	131.98	7	9
Npas1	63.7	9	9
Rangap1	63.49	8	8
Arnt	86.91	7	8
Tbl1xr1	55.63	6	8
Mark1	88.28	7	7
Safb	105.04	5	7
Wrnip1	71.75	6	7
Smarca2	180.14	6	7

B

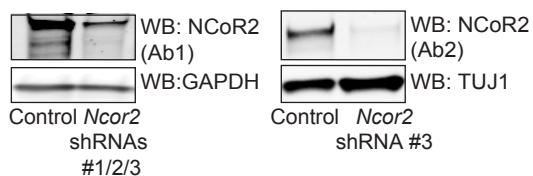


C Genomic Distribution NCoR2 Binding (Unstimulated)

D All complex component binding sites
n = 18,706Presumptive NPAS4/ARNT2 co-bound enhancers
n = 3,701

E

Wildtype Cultures



F

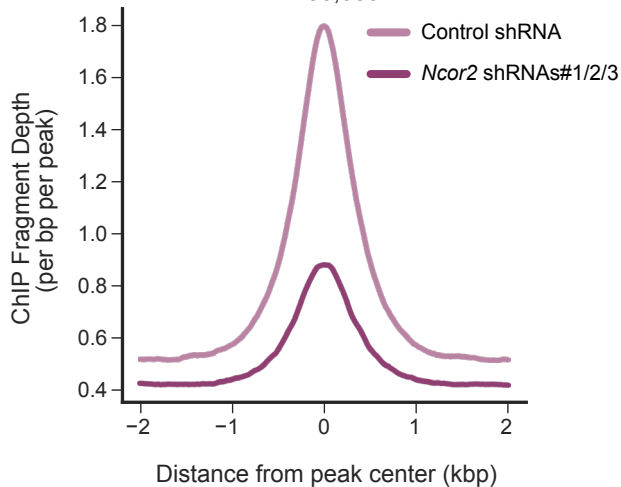
NCoR2 binding
n = 50,083

Figure S3. Related to Figure 3.

A. Ranked list of proteins recovered from IP-MS using an anti-ARNT2 IP antibody on unstimulated cortical neuron lysates. Proteins were ranked by total peptide number. Unique column displays the total number of distinct peptide sequences mapped to a given protein and total column displays the sum total of all mapping peptides.

B. STRING database visualization of top 100 ARNT2-interacting proteins in stimulated primary cortical cultures identified in at least two replicate ARNT2 purifications. Analysis required minimum confidence of association 0.4 and unconnected nodes were removed. Line thickness indicates the confidence of association.

C. Genomic distribution of NCoR2 binding sites compared to distribution of annotations by size across the genome.

D. Venn diagrams showing overlap of the NCoR2 complex components TBL1, HDAC3, and NCoR2 at all sites genome-wide (left) or at NPAS4/ARNT2-cobound enhancers (right). *** p=0, as determined by simulated sampling and intersection done with matched enhancer pools (Methods).

E. Western blot analysis confirming depletion of NCoR2 in neurons exposed to lentiviruses expressing *Ncor2* shRNAs.

F. Aggregate plot of NCoR2 ChIP-seq signal in cortical neurons transduced with control or a combination of *Ncor2* shRNAs #1,#2,#3 to demonstrate the specificity of the Thermo Fisher NCoR2 antibody (Ab 1).

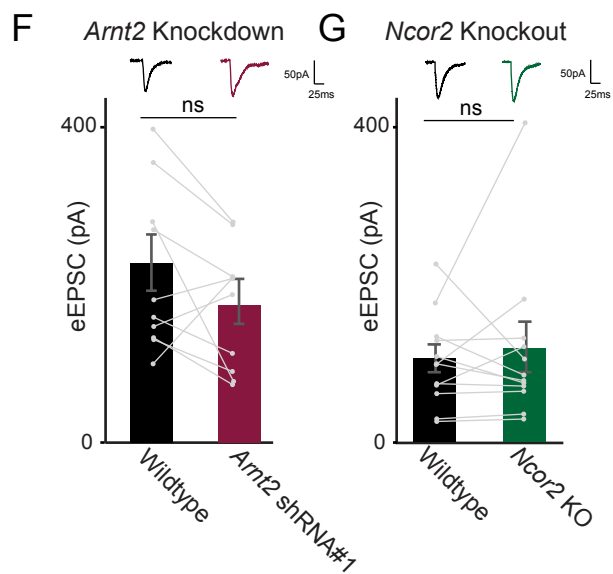
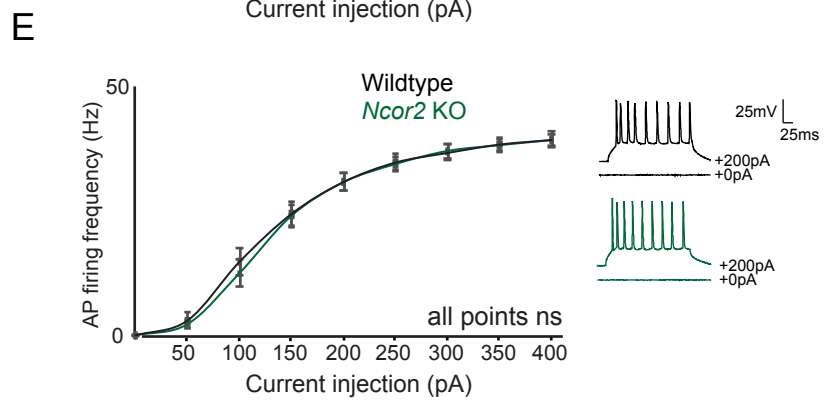
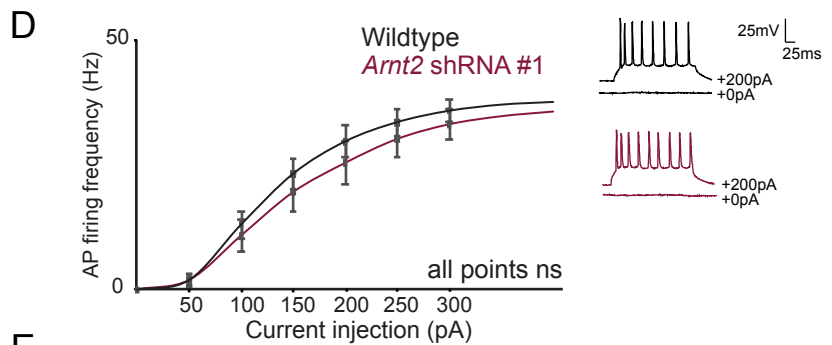
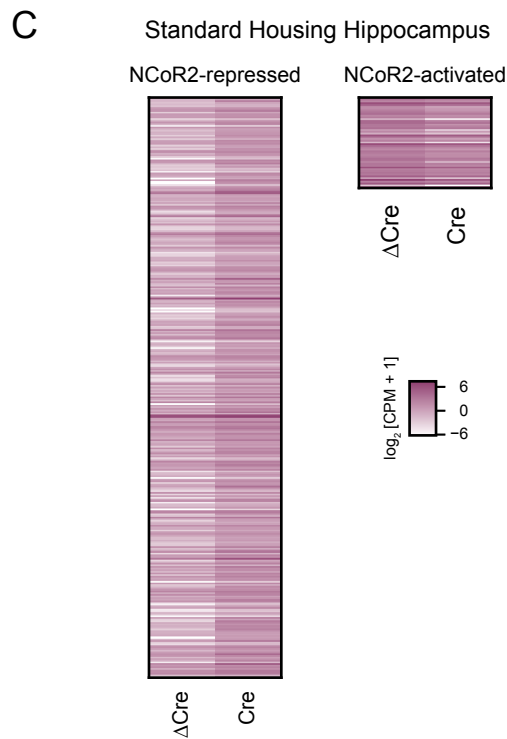
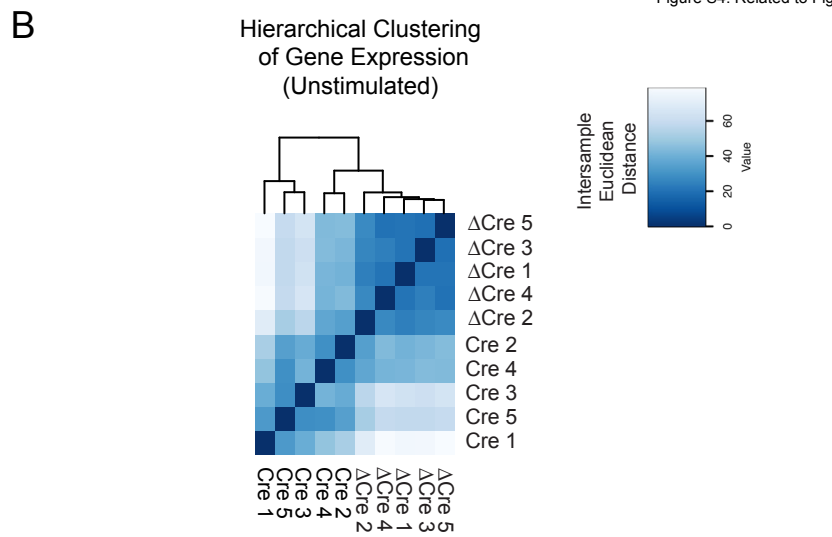
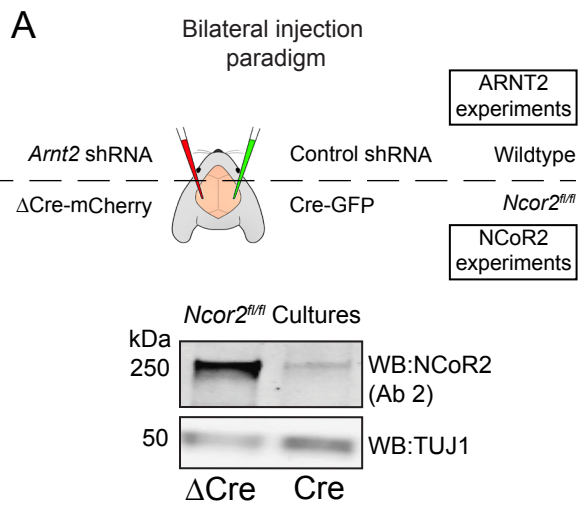


Figure S4. Related to Figure 4.

A. Top: bilateral injection scheme used for *in vivo* datasets. Within the same animal, the control hippocampal hemisphere is injected with an AAV expressing either a non-targeting, control shRNA or Δ Cre-mCherry. The contralateral hemisphere is injected with *Arnt2* shRNA #1 or Cre-GFP. Bottom: Western blot analysis confirming depletion of NCoR2 in *Ncor2^{fl/fl}* neurons exposed to lentiviruses expressing Cre or Δ Cre virus that cannot excise DNA.

B. Heatmap of Euclidean distance between all biological replicates of RNA-seq performed with hippocampal tissue following transduction with AAVs encoding Δ Cre-mCherry or Cre-GFP.

C. Heatmap of gene expression in Δ Cre-mCherry or Cre-GFP infected hippocampus displaying \log_2 expression of significantly NCoR2-repressed, (FDR < .05, fold change \geq 1.5) activity-dependent genes proximally bound by ARNT2 (\pm 10kb).

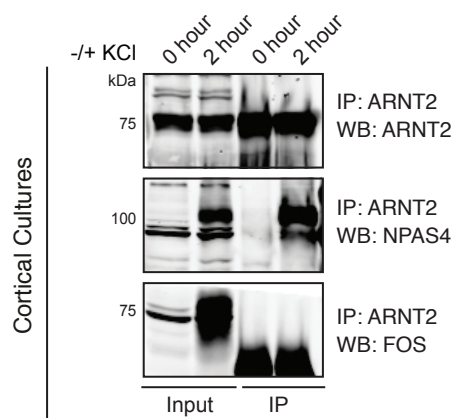
D. Current clamp recordings from wildtype or *Arnt2* shRNA-expressing neurons with current injections ranging from 0 to 400pA for 200ms in 50pA increments. Action potentials were measured and quantified. Error bars represent mean \pm SEM. ($p > 0.05$ for all current injections by ANOVA & Tukey's HSD post-hoc test)

E. Current clamp recordings from wildtype or Cre-GFP positive neurons in *Ncor2^{fl/fl}* neurons with current injections ranging from 0 to 400pA for 200ms in 50pA increments. Action potentials were measured and quantified. Error bars represent mean \pm SEM. ($p > 0.05$ for all current injections by ANOVA & Tukey's HSD post-hoc test)

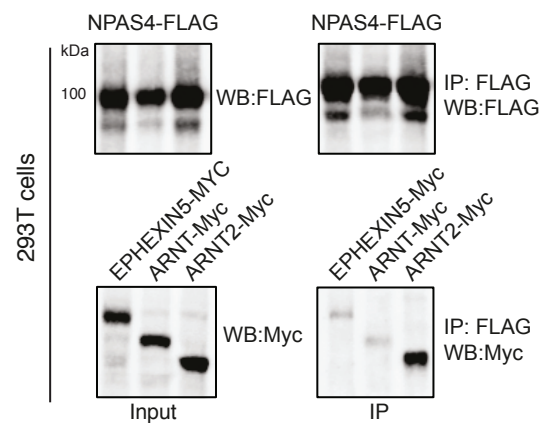
F. eEPSC amplitude simultaneously measured from wildtype, uninfected (black) and neighboring CA1 pyramidal neurons infected with an AAV expressing *Arnt2* shRNA (mCherry^{POS}, red) in response to stimulation of Schaffer collateral axons in *stratum radiatum* (*St. rad*). Individual pairs of recorded neurons are represented by paired points, with bars showing mean \pm SEM. Representative traces shown above all data. * $p < 0.05$, paired two-tailed t-test

G. eEPSC amplitude simultaneously measured from wildtype uninfected (black) and neighboring CA1 pyramidal *Ncor2^{fl/fl}* neurons infected by AAVs expressing Cre-GFP (*Ncor2-KO*, green) in response to stimulation of Schaffer collateral axons in *stratum radiatum* (*St. rad*). Individual pairs of recorded neurons are represented by paired points, with bars showing mean \pm SEM. Representative traces shown above all data. * $p < 0.05$, paired two-tailed t-test

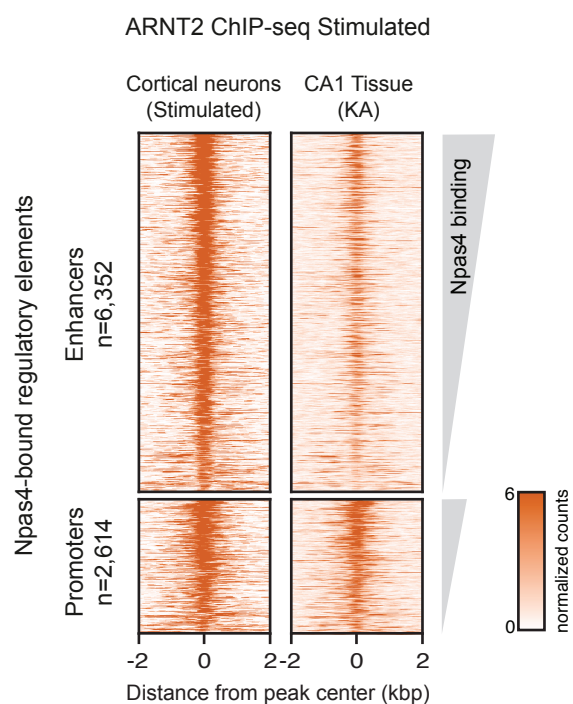
A



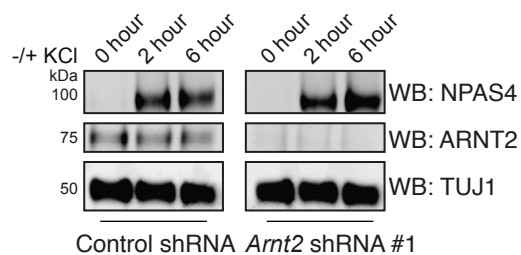
B



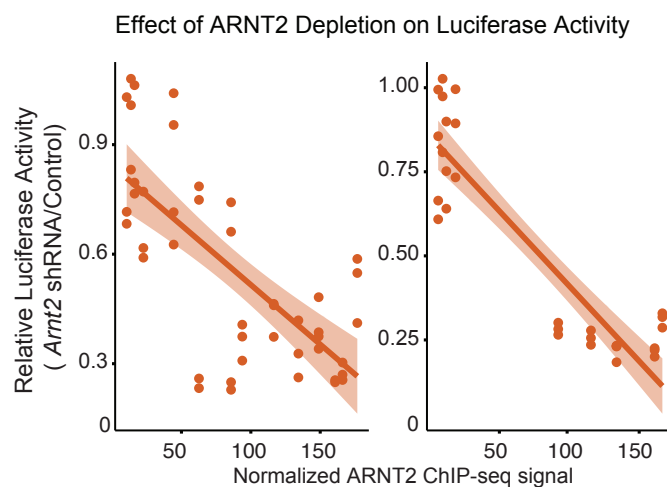
C



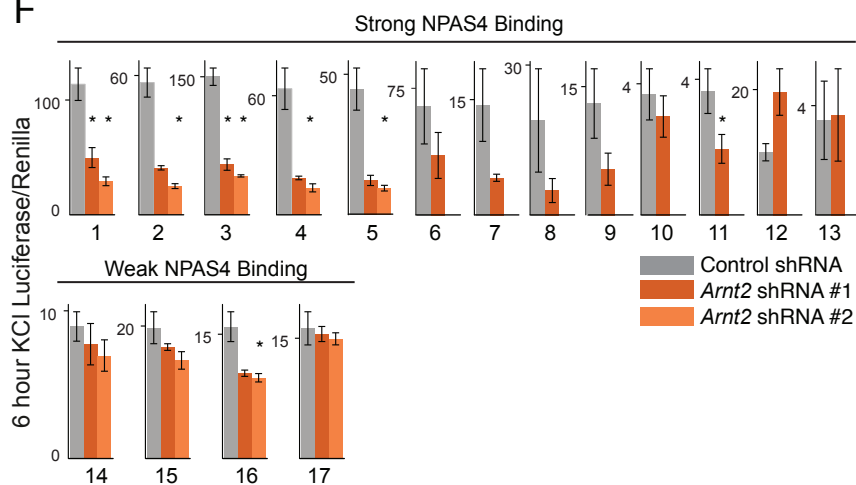
D



E



F



G

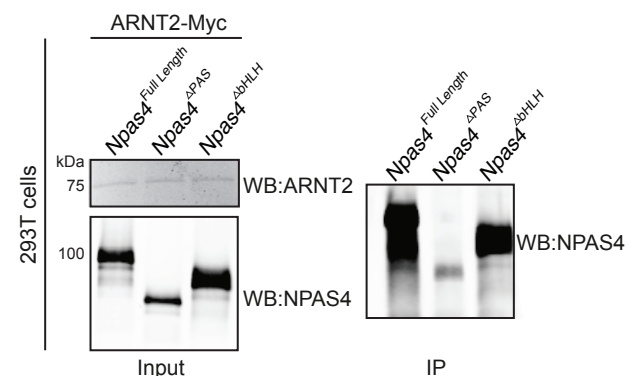


Figure S5. Related to Figure 5.

A. Western blot analysis of co-immunoprecipitations performed with anti-ARNT2 antibodies from lysates generated from unstimulated (0 KCl) or depolarized (2 KCl) cortical neurons. ARNT2 immunoprecipitates with NPAS4 but not with the immediate early gene FOS.

B. Western blot analysis of co-immunoprecipitations performed with FLAG antibodies from lysates generated from 293T cells co-transfected with NPAS4-FLAG and either ARNT-Myc, ARNT2-Myc or EPHEXIN5-Myc (as a negative control).

C. ChIP-seq signal for ARNT2 at NPAS4 sites in depolarized cortical neuron cultures (left) and CA1 hippocampal tissue derived from animals treated with the glutamatergic receptor agonist kainate (right) sorted by descending NPAS4 binding strength. Each ARNT2 binding site is represented as a single horizontal line (orange) centered at the peak summit with flanking 2kb. Color denotes ChIP-seq signal intensity (displayed in $\log_2(\text{counts per million} + 1)$). Peaks are split between enhancers bound by NPAS4 (n= 6,352) and promoters bound by NPAS4 (n = 2,614).

D. Depletion of ARNT2 by shRNA does not affect the expression levels of NPAS4 as measured by western blot analysis on neuronal lysates.

E. Effect of ARNT2 depletion on luciferase activity. Scatter plot of relative luciferase activity in 6hr KCl-depolarized neurons as a function of ARNT2 binding strength. Relative luciferase activity was calculated as the ratio of (luciferase/renilla in *Arnt2* shRNA-treated cells)/(luciferase/renilla in control shRNA-treated cells). Each point represents an independent biological replicate for a given luciferase construct (13 luciferase constructs plotted). Shaded lines indicate 95% confidence interval around line of regression. Pearson correlation: *Arnt2* shRNA#1 R = -.72 p-value = 2.9e-08; *Arnt2* shRNA#2 R = -0.92; p-value = 2e-12). Spearman correlation: *Arnt2* shRNA #1 R = -0.68; p=2.6e-07; *Arnt2* shRNA #2 R = -.86; p= 1.6e-09.

F. Luciferase activity (ratio of luciferase/renilla) of NPAS4-bound regulatory regions in KCl-depolarized neurons transfected with control shRNA or *Arnt2* shRNAs. Numbers indicate the regulatory region number (see Table S1 for genomic coordinates) and are sorted into regions where NPAS4 binds with high confidence (Strong) versus low confidence (Weak). Data are plotted as the mean \pm SEM of at least 3 independent replicates. * p < 0.05, paired, one-sided t-test with Benjamini-Hochberg multiple hypothesis correction.

G. Western blot analysis of co-immunoprecipitations performed with anti-ARNT2 antibody from 293T lysates transfected with ARNT2-myc with either NPAS4^{Full length}, NPAS4^{ΔPAS}, or NPAS4^{ΔbHLH} blotted with anti-NPAS4 antibody. The ARNT2:NPAS4 interaction is severely reduced upon deletion of PAS domains A and B from NPAS4.

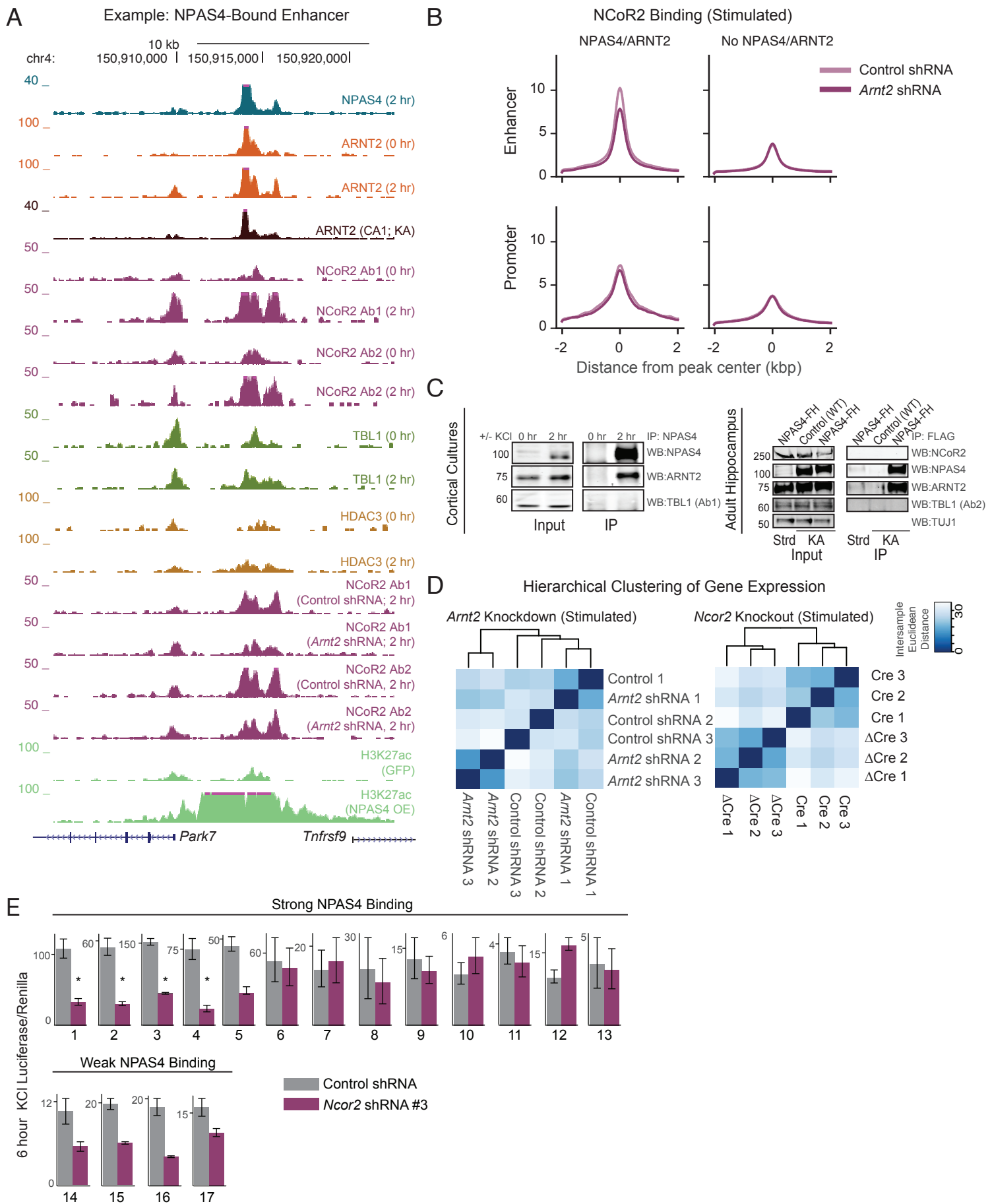


Figure S6. Related to Figure 6.

- A. Representative UCSC genome browser ChIP-seq tracks demonstrating changes to the binding of NPAS4, ARNT2, and the NCoR2 complex at an NPAS4-bound enhancer upon membrane depolarization in cortical neurons. Each ChIP-seq track is labeled by target, stimulus, and time point.
- B. Mean normalized NCoR2 ChIP-seq signal at NPAS4-bound (left) or regulatory elements not bound by NPAS4/ARNT2 (right) in membrane depolarized cultured neurons transduced with control (light line) or *Arnt2* shRNA #1 (dark line). Enhancer sites are plotted in the top panels and promoter sites are plotted in bottom panels.
- C. Left panel: Western blot analysis of co-immunoprecipitations performed with anti-NPAS4 antibodies from lysates generated from unstimulated (0 KCl) or depolarized (2 KCl) cortical neurons under these conditions. NPAS4 immunoprecipitates with ARNT2 but not with the NCoR2 complex component TBL1. Right panel: Western blot analysis of co-immunoprecipitations performed with anti-FLAG antibody from lysates generated from kainate-injected *Npas4-Flag-Ha* (*Npas4-FH*) knockin mice (described Pollina et al., in preparation). Control samples include anti-FLAG IP from kainate-injected wildtype mice that do not express NPAS4-FLAG and from saline-injected *Npas4-FH* mice, where little to no NPAS4 is expressed. NPAS4 immunoprecipitates with ARNT2 but not with TBL1 or NCoR2 under these conditions.
- D. Heatmap of Euclidean distance between all biological replicates of RNA-seq performed with hippocampal tissue following transduction with AAVS encoding control shRNA or *Arnt2* shRNA (left) or AAVs encoding Δ Cre-mCherry or Cre-GFP (right).
- E. Luciferase activity (ratio of luciferase/renilla) of NPAS4-bound regulatory regions in KCl-depolarized neurons transfected with control shRNA or *Ncor2* shRNA #3. Numbers indicate the regulatory region number (see Table S1 for genomic coordinates) and are sorted into regions where NPAS4 binds with high confidence (Strong) versus low confidence (Weak). Data are plotted as the mean \pm SEM of at least 3 independent replicates. * $p < 0.05$, paired, one-sided t-test with Benjamini-Hochberg multiple hypothesis correction.